

Original Research Article

Investigation on physical properties of carbon nanotubes prepared by mechanochemical method

Seyed Oveis Mirabootalebi*, Gholam Hosein Akbari Fakhrabadi, Reza Mirahmadi Babaheydari

Department of Materials & Metallurgy, Shahid Bahonar University of Kerman, Kerman, Iran

ARTICLE INFORMATION

Received: 19 January 2021
Received in revised: 16 March 2021
Accepted: 1 April 2021
Available online: 18 May 2021

DOI: 10.26655/AJNANOMAT.2021.3.3

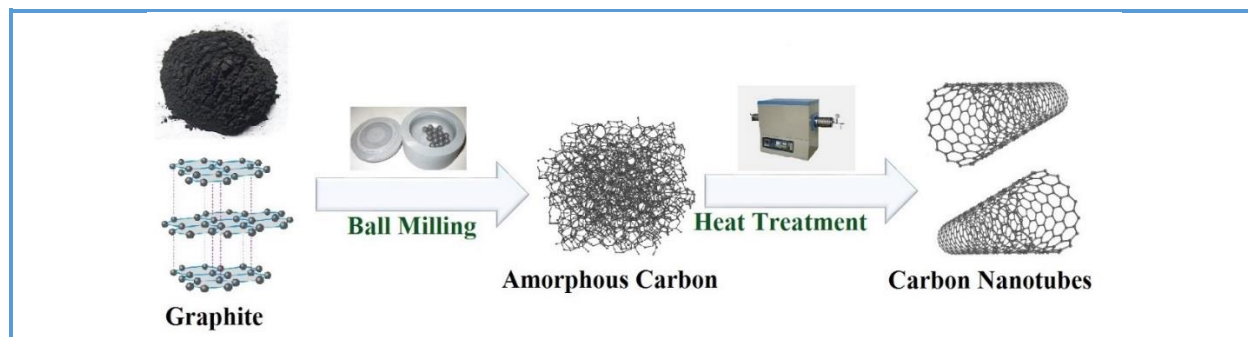
KEYWORDS

Carbon nanotubes
Mechanochemical synthesis
Optical properties
Magnetic properties

ABSTRACT

Carbon nanotubes (CNTs) have specific physical properties that make them one of the ideal nano-materials for electronics, magnetic, and optical applications. Produced CNTs via mechanochemical method have a springy and coil-like structure, affecting their physical characteristics and distinguishes them from other carbon nanotubes. In this research study, the optical and magnetic properties of fabricated carbon nanotubes by mechanochemical method were investigated. For this purpose, carbon nanotubes were synthesized by heat treatment of ball-milled graphite powders at 1400 °C in the atmosphere of argon. The quality and structure of milled-graphite and the CNTs were investigated using X-ray diffraction (XRD) analysis, scanning electron microscopy (SEM), transmission electron microscopy (TEM), atomic force microscopy (AFM) and Raman spectroscopy. Then, the optical and magnetic properties of the fabricated CNTs were assessed by UV-VIS spectrometer and vibrating-sample magnetometer (VSM), respectively. The results of the absorption spectra revealed that the products had not any absorption peak at the visible regime. Furthermore, magnetization curves indicate that coercivity (H_{ci}), magnetization (M_s), and retentivity (M_r) of the CNTs were found to be 84.183 G, 20.531, and 0.73511 emu/g, respectively. © 2021 by SPC (Sami Publishing Company), Asian Journal of Nanoscience and Materials, Reproduction is permitted for noncommercial purposes.

Graphical Abstract



Introduction

Various methods have been developed to produce nanostructured materials such as green sol-gel [1–3], hydrothermal [4], mechanochemical [5], and mechanical alloying [6]. Among these methods, the mechanochemical method is a simple and inexpensive way for the mass production of CNTs [7, 8]. This method was introduced by Chen et al. [9] and most of the produced CNTs in this process are multi-walled with a diameter of several to 100 nm and length of up to several millimeters [10–12]. Based on this method, graphite powder is firstly milled and changed to amorphous carbon, and next, the carbon nanotubes are formed in the heat treatment step [9, 13, 14]. Indeed, the milling and annealing process act as the nucleation and growth stages, respectively [15]. On the one hand, carbon nanotubes have remarkable physical properties, with various applications, including solar cells [16], LEDs [17], and MRIs [18]. Generally, most of the properties of carbon nanotubes depend on their synthesis procedure [19]. On the other hand, the optical activity of carbon nanotubes is related to their structure [20, 21]. Despite the other common methods that produce direct and aligned nanotubes [22, 23], the large majority of synthesized CNTs in the mechanochemical approach are coiled, branched, and spring-like structures [24, 25]. In spite of several studies on

the production and analysis of carbon nanotubes by the mechanochemical method, none of them focus on the general characteristics of the CNTs, especially the physical properties.

This is the first study to undertake a comprehensive analysis of the physical properties of CNTs in the mechanochemical method. In addition, an attempt was made to increase the yield of the process and quality of the products by changes in some effective variables. Milling time has a positive and direct effect on the quantity of the CNTs [11, 26]. Therefore, milling time was increased up to 330 h to increase the yield of the process. This novel step can modify the process in two distinct ways. First, maximum amorphization of carbon will produce more disorder carbonaceous precursors. Secondly, more metallic compounds of the vial are induced in the powder during mechanical alloying and they can act as the nucleation sites. To achieve a comprehensive view of the physical properties of the products, the structural, magnetic, and optical properties of the products were investigated by XRD, UV, and VSM, respectively.

Experimental

The detailed method for preparing CNTs has been described previously [25]. Briefly, elemental graphite flakes were placed in a steel vial along 5 steel balls of 15 mm in diameter, and

32 steel balls of 10 mm in diameter. The milling process was carried out in a planetary ball mill under Argon atmosphere for 330 h. In some mechanochemical methods, metal catalytic particles such as aluminum and yttrium, have been added to amorphous carbon to facilitate the fabrication of carbon nanotubes [27, 28]. However, in this work, no catalysts were used to reduce the proportion of metal impurities. Indeed, just the metal particles that enter the powder during the ball-milling act as preferred sites for nucleation and growth of CNTs. Next, by heat treatment of milled-graphite at 1400 °C in the atmosphere of Argon, carbon nanotubes were fabricated. In the final stage, synthesized CNTs were subjected to thermal purification under the air atmosphere at the temperature of 330 °C for 132 min.

Figure 1 illustrates the schematic diagram of the process for the fabrication of the CNTs. An X-ray diffractometer (Philips X'Pert, Cu-K α ,

$\lambda=0.1542$ nm) was used to investigate the crystallographic structures of samples. These XRD profiles were analyzed by Rietveld refinement and MAUD (Material Analysis Using Diffraction) to estimate the proportion of the produced amorphous phase, crystallite size, d-spacing, and micro-strain. Morphology and size of milled-graphite particles were characterized by using scanning electron microscopy (Cam Scan mv2300). Atomic force microscope (Autoprobe Cp, contact mode, 1 Hz rate of scan) and transmission electron microscopy (LEO912-AB operated at 100 kV) were used to study the structure of produced CNTs. The quality and type of CNTs were analyzed by Raman spectroscopy (Takram P50C0R10, excited at 532 nm). To study the optical and magnetic properties of the products, UV-Visible Spectroscopy (STM UV 9000) and Vibrating-sample magnetometer (Lake Shore Cryotronics-7407) were used, respectively.

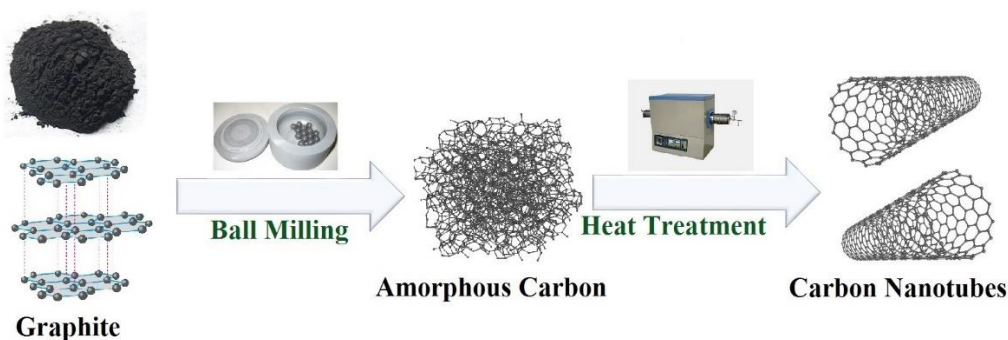


Figure 1. Graphical abstract of the process for preparing the CNTs

Results and Discussion

The X-ray diffraction patterns of graphite powder for various activation times are depicted in Figure 2. There are several techniques for qualitative and quantitative analysis of XRD profiles such as the Debye-Scherrer equation and Williamson-Hall [29, 30]. In this work, we used Rietveld refinement and MAUD based on the correction of the least-

squares. This approach is one of the advanced methods for analyzing X-ray diffraction patterns and calculation of the crystallographic parameters [31]. Regarding the XRD patterns in Figure 2, the proportions of the produced amorphous phases and important crystallographic properties of carbon were measured by MAUD/ Rietveld and placed in Table 1. Unmilled graphite has a sharp peak at 26°-27° and a broad peak at 43°-46°. These

peaks become broader and shorter by increasing the milling time. This is due to enhance of the surface area of graphite particles, the development of dislocations, and create sub-grain boundaries. The hexagonal structure of graphite changed to the amorphous structure if the grain size of graphite is reduced to about 3 nm. This is related to the destruction of the crystalline structure and the decrease in the grain and crystallite size of graphite [9]. In the previous studies [32, 33], it has been reported after about 170-1000 h of graphite milling, no changes in the XRD pattern have been observed. This is owing to a balance between recovery and recrystallization and dislocation motion [34]. Generally, when the graphite particles achieve the minimum crystallite size, due to the strong σ bond and high flexibility of the graphite plates, they are

bent and transformed to new structures, instead of changing the crystallite size. These structures including ribbon nanostructures [35], spherical and crystal structures of graphite [36], and carbon microtubes and nanotubes [36–39].

Figure 3 shows the SEM images of the graphite powder before and after the MA. As the milling time increases, the graphite particles become more and more small and spherical. However, powders were joined to larger particles, and their surface areas enhanced after agglomeration. This increase in surface energy can lead to the formation of a suitable raw material for the preparation of CNTs. As milling time has a direct and positive effect on the efficiency of production of carbon nanotubes [24].

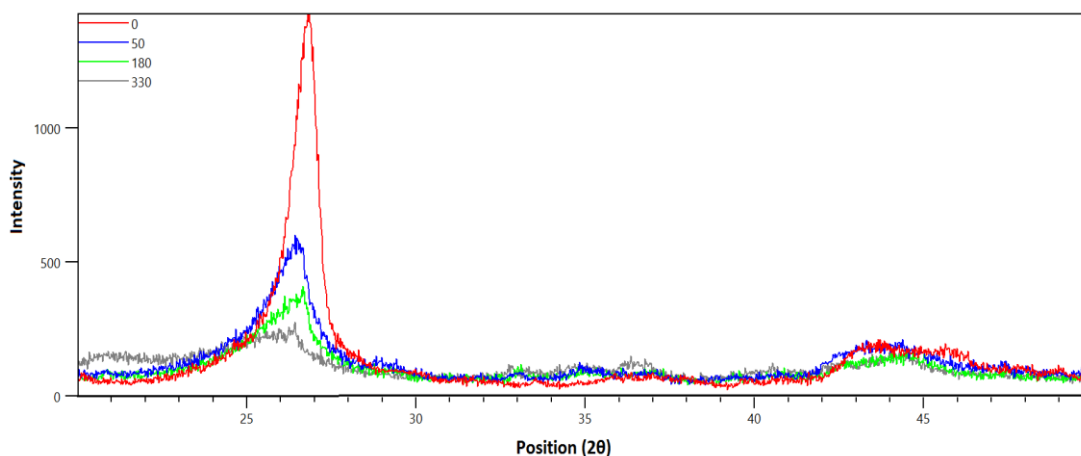


Figure 2. XRD pattern of ball-milled graphite at different milling times

Table 1. Characteristics of the crystal structure of graphite during the ball-milling process

Amorphous percentage	Crystallite Size (nm)	d_{002} (nm)	Micro strain	Milling Time (h)
0	390	0.332	0.00613	0
69	58	0.337	0.0219	100
72	50.92	0.3376	0.0223	180
93	1.3	0.339	0.02507	330

TEM and AFM images of synthesized CNTs after the heat treatment of milled-graphite and

thermal purification are illustrated in Figure 4. These CNTs are coiled and branched in different

lengths and diameters. This unique appearance of the produced carbon nanotubes is one of the special features of this method which have been observed previously [40]. Diverse dimensions and indirect structures of carbon nanotubes were attributed to the distribution of metal catalysts and the competition between carbon atoms to create hexagons, heptagonal, and pentagons [41]. So, produced CNTs in

mechanochemical are spring-like and have a peculiar structure.

Based on the nucleation and the growth mechanism for synthesizing carbon nanotubes in the presence of catalyst [42, 43] the production of CNTs performs on catalytic particles. By reducing the solubility and deposition of carbon atoms in the solution of carbon atoms and the metal catalysts, carbon

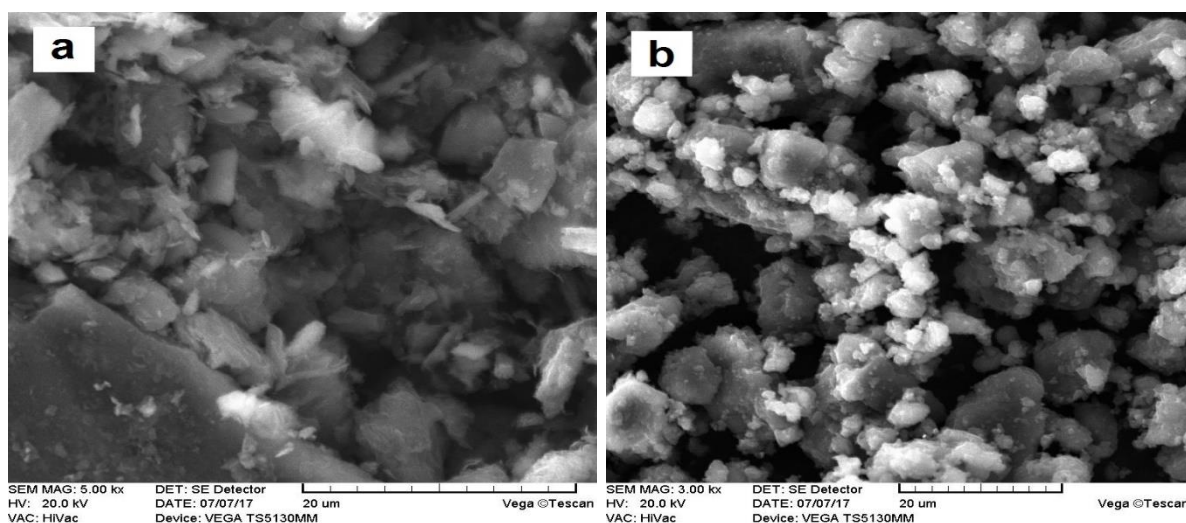


Figure 3. SEM images of a) graphite before and b) after the mechanical milling

atoms by sp^2 bonds are connected and finally make the structure of carbon nanotubes. According to this mechanism, it can be expected that the diameter of the catalyst directly affects the diameter of the produced carbon nanotubes, as many reports [44] experimentally pointed out a decrease in the diameter of the nanotubes through increasing the milling time. The diameter and indirect structure of carbon nanotubes play a major role in the physical properties of the CNTs by affecting their electronic structure and topology.

Raman spectroscopy was carried out for the more accurate study of the structure and quality of the synthesized carbon nanotubes. The Raman spectrum in Figure 5 exhibits three sharp peaks centered at 1349, 1566, and 2650 cm^{-1} , assigned to D, G, and G' bands,

respectively. The existence of the G-single-band (without Splitting) in Figure 5 is a strong sign of the presence of multi-walled carbon nanotubes (MWCNTs). Non-split between G+ and G- bands owing to the variant groups of MWCNTs and the difference in the distribution of diameters of each multi-walled carbon nanotube, lead to a single band of G [45]. Low-frequency peaks in radial breathing mode ($100-200\ cm^{-1}$) related to the inner diameter of carbon nanotubes (more than 2 nm) and the number of walls (more than 20) which make peaks extremely weak and invisible [46–48]. These weak peaks in this region indicate a relatively small percentage of single-walled carbon nanotubes (SWCNTs). D-band shows the disorders and asymmetry in the crystallographic structure of graphite plates such as impurities, porosity, and defect which

are present in carbon structures with sp^2 bonds [49]. The long-range order of the CNTs can be determined by the G'-band. This band corresponds to the two-phonon process and its intensity depends on the purity of the sample [50]. Accordingly, ID/IG' can be used as a sensitive parameter to specify the impurities of CNTs. However, this factor is less important than ID/IG for estimating the quality of carbon nanotubes [51]. In the vast majority of previous

studies, acid purification was performed before Raman spectroscopy [32, 40], which can significantly increase the quality of the produced nanotubes. In this study, acid leaching was not performed to achieve a more realistic perception of the quality and optical properties of the CNTs. Hence, the obtained ID/IG (0.79) and ID/IG' (1.21) confirm ordered sp^2 bonds and suitable graphitization and quality of the CNT.

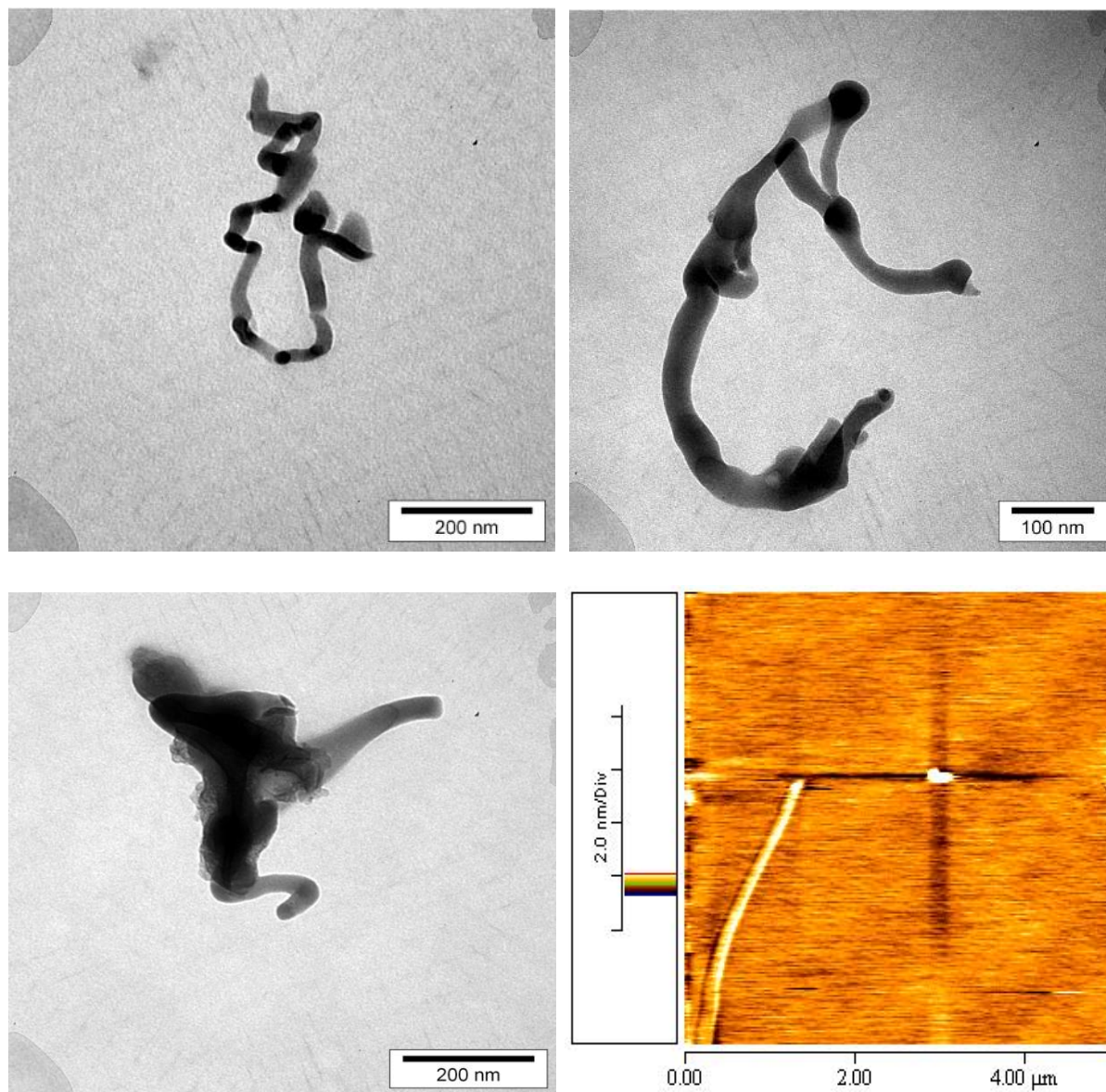


Figure 4. TEM and AFM images of ball-milled graphite after the heat treatment at 1400 °C

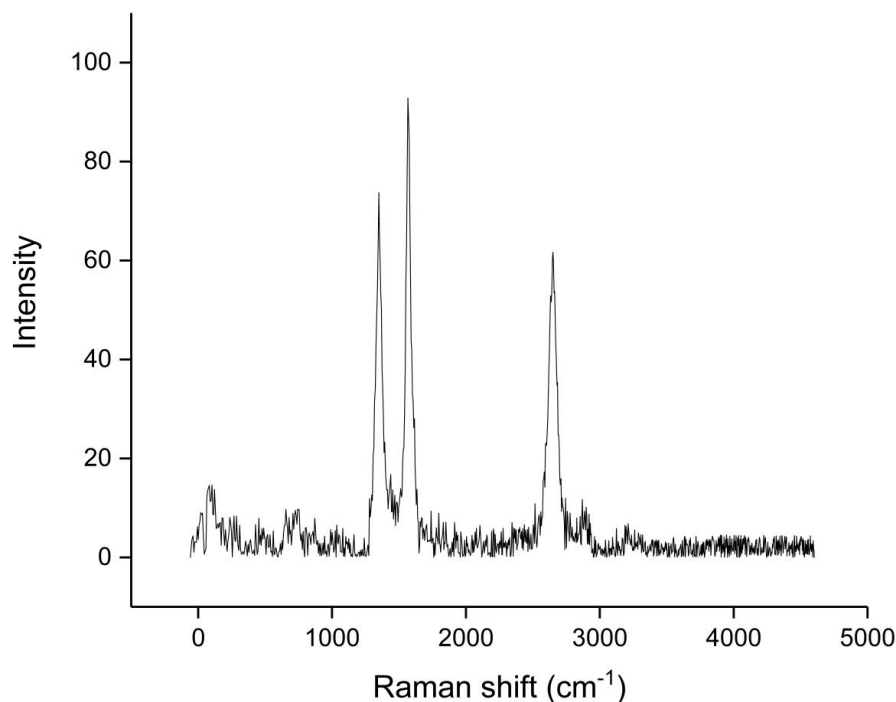


Figure 5. Raman spectrum of synthesized carbon nanotubes after thermal purification

Figure 6 provides information about the X-ray diffraction pattern of the generated CNTs. There is a sharp and broad peak in the range of 26° and 43° , respectively. In general, the (002) peak is weakened, broadened, and shifted to the left by about half a degree from 26.5 to 26° in the XRD pattern of carbon nanotubes. This is owing to the number of walls, changes in the interlayer space, lattice distortion, and the orientation of the CNTs against X-rays [52]. The interlayer distance (d_{002}) in multi-walled carbon nanotubes is usually 0.34 nm [53]. According to XRD profiles, d_{002} for primary graphite and CNTs is 3.32 and 3.42 Å, respectively. The d_{002} is increased by decreasing the diameter of the carbon nanotubes due to differences in the reflection of straight and curved plates [54–56]. In other words, the interlayer distance in CNTs is slightly greater than the interplanetary distance in pure graphite.

Furthermore, the diameter of the first wall in MWCNTs is often more than 2 nm [41]. Since the

number of walls usually has a one-to-one relationship with the diameter of multi-walled carbon nanotubes [53], it can be estimated that there are 20 to 50 walls in the generated carbon nanotubes with 20 nm in diameter in Figure 4

UV-VIS absorption spectroscopy of carbon nanotubes after the thermal purification is depicted in Figure 7. There is no peak except a sharp peak at 200 – 250 nm and transitions and excitation of electrons just happen at 210 nm. This absorption band is attributed to plasmon resonances in the free electron cloud and the π – π^* interactions [57, 58]. According to John et al. [59], the optical band-gap in the visible region of the carbon nanotubes is greater than graphite and so absorbance was performed only at the limited wavelengths. This phenomenon is probably due to the curvature of the graphene plates, the bending in the molecular hybrid orbitals, and the effect of the nonmetric radius of the carbon nanotubes. Defects can affect the optical properties of CNTs by decreasing

fluorescence efficiency [60]. However, the obtained absorption peak in the UV region shows that the indirect and spring-like structures of the carbon nanotubes have not a significant effect on the light absorption of the

carbon nanotubes in the mechanical method. Accordingly, this absorption peak is in good agreement with the results of the previous studies of UV-VIS spectra of another type of CNTs [61–64].

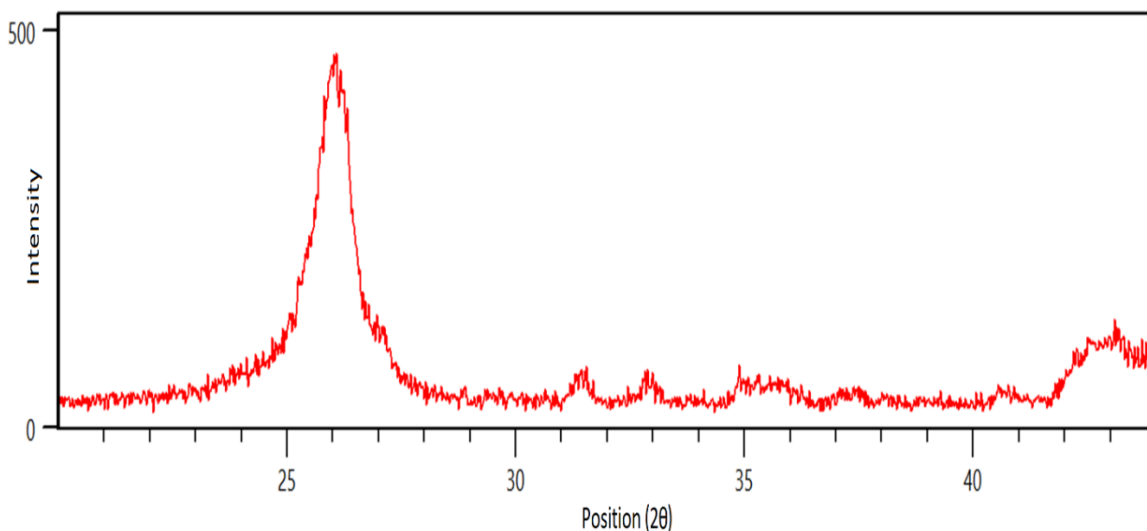


Figure 6. XRD diffraction pattern of the produced carbon nanotubes after the purification process

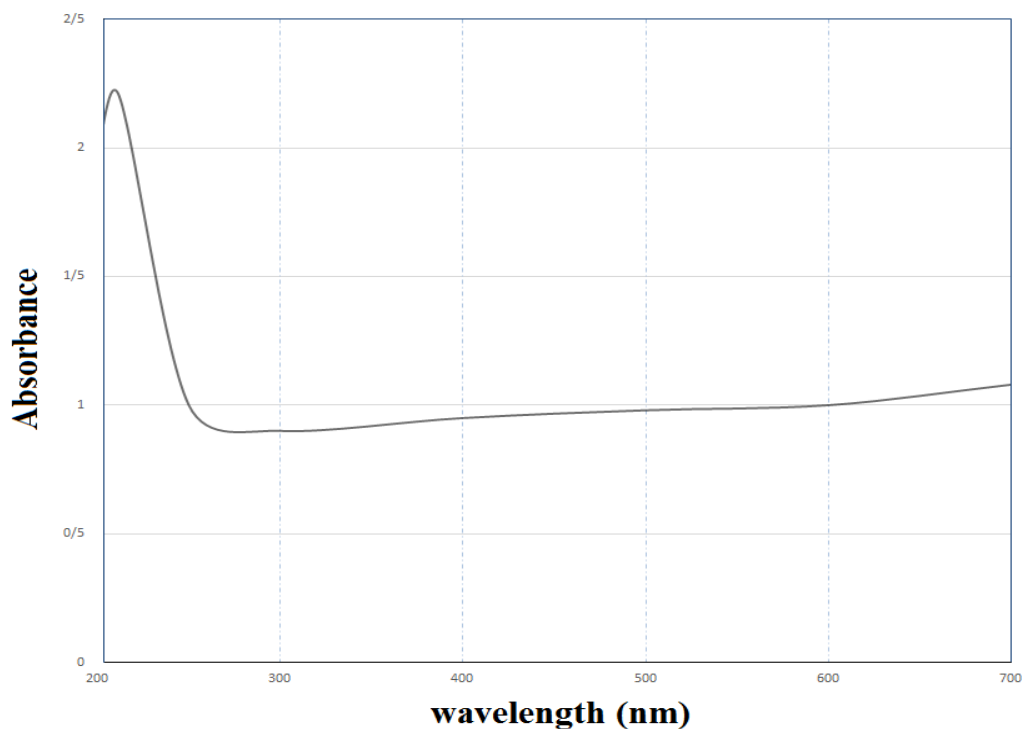


Figure 7. UV-VIS absorption spectroscopy of the carbon nanotubes synthesized by annealing the ball-milled graphite after thermal purification

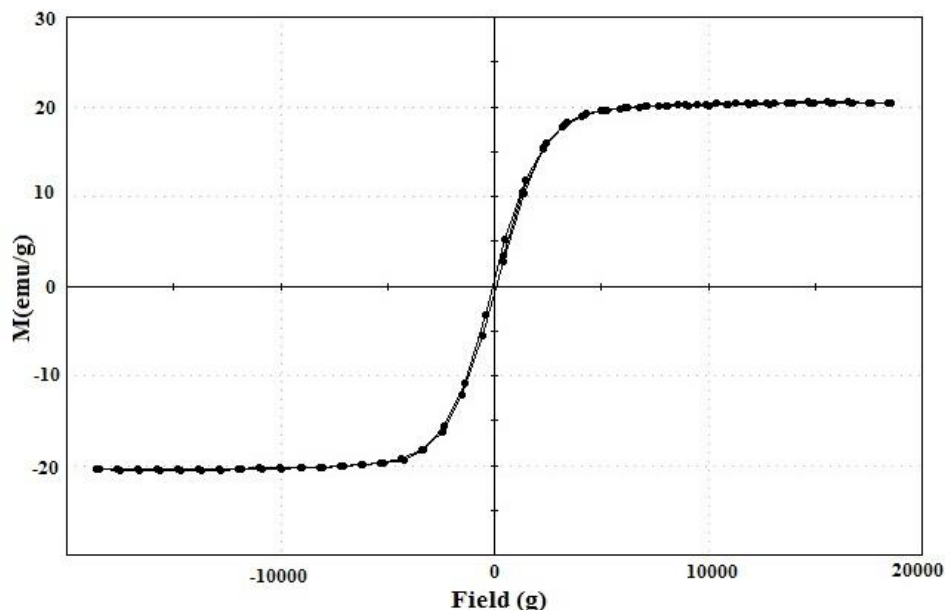


Figure 8. The magnetization curves of fabricated CNTs

VSM analysis of produced CNTs is demonstrated in Figure 8. Coercivity (H_{ci}), magnetization (M_s), and retentivity (M_r) of the CNTs are 84.183 G, 20.531 emu/g, and 0.73511 emu/g, respectively. Generally, the magnetic properties of carbon nanotubes depend on various factors, and one of the most important parameters is the quality and structure of the CNTs [65]. The mechanochemical method, due to high temperature and high-energy ball-milling during a long time of the process, can reduce the quality of synthesized carbon nanotubes by the destruction of CNT's structure. For example, injected shock power (which was in the range of 1-2 W/g in this study according to the Suryanarayana curve [34]), or metal impurities during ball-milling can disrupt the magnetic properties of the CNTs. Apparently, springy and coil-like structures have not any impact on the magnetic properties of the products. VSM results represent the soft magnetic property of the carbon nanotubes and the hysteresis loop of the products indicates the energy loss per cycle is small. As a result, in some electronic devices like transistors, which require little loss of

hysteresis because of the frequent reverse flow [66–68], synthesized products can be a very good option.

Conclusions

In this work, after the heat treatment of ball-milled graphite powder, carbon nanotubes were produced and their optical and magnetic properties were investigated. Two main peaks were identified in the range of 26° and 43° of the X-ray diffraction pattern analysis of the CNTs. The results of the UV-VIS spectroscopy analysis demonstrated that the absorption was only in the ultraviolet region (200-250 nm). In addition, the results of the VSM revealed that the synthesized nanotubes have completely soft magnetic properties with a very small hysteresis curve and energy loss per cycle. According to the magnetization curves, coercivity (H_{ci}), magnetization (M_s), and retentivity (M_r) of the CNTs were 84.183 G, 20.531 emu/g, and 0.73511 emu/g, respectively.

Disclosure Statement

No potential conflict of interest was reported by the authors.

References

- [1]. Moradnia F., Fardood S.T., Ramazani A., Min B.K., Joo S.W., Varma R.S. *Journal of Cleaner Production*, 2021, **288**:125632
- [2]. Taghavi Fardood S., Moradnia F., Ghalaichi A.H., Danesh Pajouh S., Heidari M. *Nanochemistry Research*, 2020, **5**:69
- [3]. Fardood S.T., Forootan R., Moradnia F., Afshari Z., Ramazani A. *Materials Research Express*, 2020, **7**:015086
- [4]. Ajormal, F., Moradnia F., Taghavi Fardood S., Ramazani A. *Journal of Chemical Reviews*, 2020, **2**:90
- [5]. Boyrazlı M., Güler S.H. *Journal of Molecular Structure*, 2020, **1199**:126976
- [6]. Mirahmadi Babaheydari R., Mirabootalebi S.O., Akbari Fakhrabadi G.H. *Iranian Journal of Materials Science & Engineering*, 2021, **18**:1
- [7]. Mirabootalebi S.O. Fakhrabadi G.H.A. *Int. J. Bio-Inorg. Hybr. Nanomater*, 2017, **6**:49
- [8]. Manafi S., Amin M., Rahimipour M., Salahi E., Kazemzadeh A. *Advances in Applied Ceramics*, 2010, **109**:25
- [9]. Chen Y., Fitz Gerald J., Chadderton L.T., Chaffron L. *Applied Physics Letters*, 1999, **74**:2782
- [10]. Manafi S., Rahimipour M.R., Mobasherpour I., Soltanmoradi A. *Journal of Nanomaterials*, 2012, **2012**:15
- [11]. Chen Y., Conway M., Fitzgerald J. *Applied Physics A*, 2003, **76**:633
- [12]. Manafi S., Rahimipour M., Soltanmoradi A. *Materials Science-Poland*, 2012, **30**:226
- [13]. Chen Y., Fitz Gerald J., Chadderton L., Chaffron L. *Journal of Metastable and Nanocrystalline Materials*, 1999, **2-6**:375
- [14]. Smeulders D., Milev A., Kannangara G.K., Wilson M. *Journal of Materials Science*, 2005, **40**:655
- [15]. Chen Y., Li C.P., Chen H., Chen Y., *Science and Technology of Advanced Materials*, 2006, **7**:839
- [16]. Cui K., Maruyama S. *Progress in Energy and Combustion Science*, 2019, **70**:1
- [17]. Yan C., Lu H., Li Z., Li J., Tang Y., Yu B. 16th China International Forum on Solid State Lighting & 2019 International Forum on Wide Bandgap Semiconductors China (SSLChina: IFWS). 2019. IEEE
- [18]. Wang S., Lin Q., Chen J., Gao H., Fu D., Shen S. *Carbon*, 2017, **112**:53
- [19]. Guldi D.M., Martín N. *Carbon nanotubes and Related Structures: Synthesis, Characterization, Functionalization, and Applications*. 2010: John Wiley & Sons
- [20]. Mahajan D. *Asian Journal of Applied Science and Technology*, 2017, **1**:15
- [21]. Ezzatzadeh E. *Asian Journal of Nanoscience and Materials*, 2021, **4**:125
- [22]. Thapa A., Neupane S., Guo R., Jungjohann K.L., Pete D., Li W. *Diamond and Related Materials*, 2018, **90**:144
- [23]. Karthikeyan K., Angulakshmi V., Karthikeyan S., Jothivenkatachalam K., Kumar P.A. *Bulletin of the Chemical Society of Ethiopia*, 2017, **31**:233
- [24]. Güler Ö., Evin E. *Fullerenes, Nanotubes and Carbon Nanostructures*, 2015, **23**:463
- [25]. Mirabootalebi S. *Advanced Composites and Hybrid Materials*, 2020, **3**:336
- [26]. Evin E., Güler Ö., Aksoy M., Güler S.H. *Bulletin of Materials Science*, 2015, **38**:857
- [27]. Connan H.G., Reedy B.J., Marshall C.P., and Wilson M.A. *Energy & Fuels*, 2004, **18**:1607
- [28]. Rosas G., Esparza R., Liu H., Ascencio J., Pérez R. *Materials Letters*, 2007, **61**:860
- [29]. Moradnia F., Fardood S.T., Ramazani A., Osali S., Abdolmaleki I. *Micro & Nano Letters*, 2020, **15**:674
- [30]. Taghavi Fardood S., Moradnia F., Moradi S., Forootan R., Yekke Zare F., and Heidari M. *Nanochemistry Research*, 2019, **4**:140

- [31]. Lutterotti L. *Acta Crystallogr. A*, 2000, **56**:s54
- [32]. Manafi S., Amin M., Rahimipour M., Salahi E., and Kazemzadeh A. *New Carbon Materials*, 2009, **24**:39
- [33]. Welham N. Williams J. *Carbon*, 1998, **36**:1309
- [34]. Suryanarayana C. *Progress in Materials Science*, 2001, **46**:1
- [35]. Huang Z., Calka A., Liu H. *Journal of Materials Science*, 2007, **42**:5437
- [36]. Chen X., Yang H., Wu G., Wang M., Deng F., Zhang X., Peng J., and Li W. *Journal of Crystal Growth*, 2000, **218**:57
- [37]. Li J., Wang L., Bai G., Jiang W. *Scripta Materialia*, 2006, **54**:93
- [38]. Huang J., Yasuda H., Mori H. *Chemical Physics Letters*, 1999, **303**:130
- [39]. Li J., Peng Q., Bai G., Jiang W. *Carbon*, 2005, **13**:2830
- [40]. Manafi S., Rahimipour M., Pajuhanfar Y. *Ceramics International*, 2011, **37**:2803
- [41]. Lehman J.H., Terrones M., Mansfield E., Hurst K.E., Meunier V. *Carbon*, 2011, **49**:2581
- [42]. Purohit R., Purohit K., Rana S., Rana R., Patel V. *Procedia Materials Science*, 2014, **6**:716
- [43]. Kumar M. Ando Y. *Journal of Nanoscience and Nanotechnology*, 2010, **10**:3739
- [44]. Chen Y., Conway M., Fitzgerald J. *Applied Physics A: Materials Science & Processing*, 2003, **76**:633
- [45]. Costa S., Borowiak-Palen E., Kruszynska M., Bachmatiuk A., Kalenczuk R. *Materials Science-Poland*, 2008, **26**:433
- [46]. Benoit J., Buisson J., Chauvet O., Godon C., Lefrant S. *Physical Review B*, 2002, **66**:073417
- [47]. Zdrojek M., Gebicki W., Jastrzebski C., Melin T., Huczko A. *Solid State Phenomena*. 2004, **99**:265
- [48]. Lefrant S. *Current Applied Physics*, 2002, **2**:479
- [49]. Antunes E., Lobo A., Corat E., Trava-Airoldi V. *Carbon*, 2007, **45**:913
- [50]. DiLeo R.A., Landi B.J., Raffaele R.P. *Journal of Applied Physics*, 2007, **101**:064307
- [51]. Chakrapani N., Curran S., Wei B., Ajayan P.M., Carrillo A., Kane R.S. *Journal of Materials Research*, 2003, **18**:2515
- [52]. Chen P., Wu X., Sun X., Lin J., Ji W., Tan K. *Physical Review Letters*, 1999, **82**:2548
- [53]. Chiodarelli N., Richard O., Bender H., Heyns M., De Gendt S., Groeseneken G., Vereecken P.M. *Carbon*, 2012, **50**:1748
- [54]. Kiang C.-H., Endo M., Ajayan P., Dresselhaus G., Dresselhaus M. *Physical Review Letters*, 1998, **18**:1869
- [55]. Onyestyák G., Valyon J., Hernádi K., Kiricsi I., Rees L. *Carbon*, 2003, **41**:1241
- [56]. Singh D.K., Iyer P., Giri P. *Diamond and Related Materials*, 2010, **19**:1281
- [57]. Tasaki S., Maekawa K., Yamabe T. *Physical Review B*, 1998, **57**:9301
- [58]. Jeong M.S., Byeon C.C., Cha O.H., Jeong H., Han J.H., Choi Y.C., An K.H., Oh K.H., Kim K.K., Lee Y.H. *Nano*, 2008, **3**:101
- [59]. Johan M.R. Moh L.S. *Carbon*, 2013, **8**:1047
- [60]. Cherukuri T.K., Tsyboulski D.A., Weisman R.B. *ACS Nano*, 2012, **6**:843
- [61]. Johan M.R. Moh L.S. *Int. J. Electrochem. Sci*, 2013, **8**:1047
- [62]. Fathi Z., Nejad R.-A.K., Mahmoodzadeh H., Satari T.N. *Journal of Plant Protection Research*, 2017, **57**:228
- [63]. Shende R.C. Ramaprabhu S. *Solar Energy Materials and Solar Cells*, 2016, **157**:117
- [64]. Zawadzka A., Płóciennik P., Korcala A., Szroeder P. *Optical Materials*, 2019, **96**:109295
- [65]. Farahmandjou M., Khalili P. *Asian Journal of Green Chemistry*, 2021, **5**:219
- [66]. Liu J.P., Fullerton E., Gutfleisch O., Sellmyer D.J., *Nanoscale Magnetic Materials and Applications*, 2009; p XXIV, 719
- [67]. Dekker C. *Nature Electronics*, 2018, **1**:518
- [68]. Jeong Y.J., Bae J., Nam S., Lim S., Jang J., Kim S.H., Park C.E. *Organic Electronics*, 2016, **39**:272

How to cite this manuscript: Seyed Oveis Mirabootalebi*, Gholam Hosein Akbari Fakhrabadi, Reza Mirahmadi Babaheydari. Investigation on physical properties of carbon nanotubes prepared by mechanochemical method. *Asian Journal of Nanoscience and Materials*, 4(3) 2021, 201-212. DOI: 10.26655/AJNANOMAT.2021.3.3